Perpendicular magnetic fields in cantilever beam magnetometry

R. Koch,[a] A. K. Das,[b] H. Yamaguchi,[c] C. Pampuch,[d] and A. Ney[e]
Paul-Drude-Institut für Festkörperelektronik, Hausvogteiplatz 5-7, D-10117 Berlin, Germany

(Received 10 February 2004; accepted 11 June 2004)

Cantilever beam magnetometry is a common technique to determine the magnetoelastic (ME) coupling constants of thin films by measuring the stress that develops when the film magnetization is changed. In cantilever beam experiments performed so far the film magnetization was mainly rotated within the film plane. Here we discuss the measurement of the ME coupling constants, when the magnetizing field is chosen so that it rotates the film magnetization out of the film plane. A major stress contribution, which arises additionally to the ME stress, originates in the torque that magnetic dipoles experience in a magnetic field. In order to separate torque effects from ME contributions in cantilever beam experiments a general method is proposed. With this method the ME coupling constants can be quantitatively determined and furthermore the film magnetization as well as its perpendicular anisotropy constant are obtained quantitatively. © *2004 American Institute of Physics*. [DOI: 10.1063/1.1778479]

I. INTRODUCTION

In magnetic materials, a change in the state of magnetization (direction and/or magnitude), by any means (e.g., magnetic field or temperature) changes the state of the lattice (size and/or shape) and vice versa. This phenomenon is well known as magnetostriction and can be quantified either via the magnetoelastic (ME) coupling constants B_i or the magnetostrictive constants λ_i, both related via the elastic constants.[1,2] The free energy F of a magnetic material contains two contributions depending on strain (ϵ), the elastic energy F_{el}, and the ME energy F_{mel}. A change in one energy, F_{el} or F_{mel}, induces the other one to minimize F. In the bulk, typical ME strain is 10^{-5}–10^{-4} and corresponds to negligibly small changes in $F_{\mathrm{mel}} \sim B\epsilon$ compared to other magnetic contributions (e.g., magnetocrystalline energy or magnetostatic energy). On the other hand, in case of heteroepitaxial thin films, the intrinsic distortion due to lattice mismatch between film and substrate usually amounts to strain of several percent ($\epsilon \approx 10^{-2}$), thus affecting F_{mel} substantially. Therefore the ME coupling plays an important role in the case of highly strained heteroepitaxial systems.

The experimental determination of the ME coupling effect is not straightforward. Various experimental methods have been developed in the past for investigating the ME properties of thin films.[3] Indirect methods are based on the stress (externally applied by pressing, stretching, or bending the samples) dependence of the magnetic properties[4] such as susceptibility or ferromagnetic resonance frequency. The main idea of these indirect methods is to exploit the contribution of the ME coupling to the magnetic anisotropy. A very convenient and rapid method to measure directly the sign and the magnitude of the ME coupling has been introduced as early as 1976 by Klokholm,[5] who determined the deflection of the end of a cantilever beam coated by a ferromagnetic film, when changing the direction of magnetization. In the cantilever beam experiments performed so far the film magnetization was mainly rotated within the film plane.[5–10] The respective analysis of the deflection data to obtain the magnetostriction constants has been subject of many studies.[7,11–16]

Here we address some of the peculiarities involved in measuring the ME coupling constants with a cantilever beam magnetometer[7] (CBM), when the magnetizing field is chosen so that it rotates the film magnetization out of the film plane. A major stress contribution arising then in addition to the ME stress originates in the torque that magnetic dipoles experience in a magnetic field. In order to separate torque effects from ME contributions in cantilever beam experiments a general method is proposed. We will show that by applying this method the ME coupling constants as well as the magnetization and the perpendicular anisotropy constant of the film can be determined quantitatively. This method is discussed by means of an epitaxial MnAs film on GaAs(001).

II. DESIGN OF EXPERIMENT

For evaluation of the CBM results of the hexagonal MnAs film, the following equations for F_{el} and F_{mel} have been derived by Legendre transformation of the expression for the free energy of a hexagonal crystal given by Mason:[17]

$$F_{\mathrm{el}} = \tfrac{1}{2}c_{11}(\epsilon_1^2 + \epsilon_2^2) + c_{12}\epsilon_1\epsilon_2 + c_{13}\epsilon_3(\epsilon_1 + \epsilon_2) + \tfrac{1}{2}c_{33}\epsilon_3^2 + \tfrac{1}{2}c_{44}(\epsilon_4^2 + \epsilon_5^2) + \tfrac{1}{4}(c_{11} - c_{12})\epsilon_6^2, \quad (1)$$

$$F_{\mathrm{mel}} = B_1[(\alpha_1^2 - 1)\epsilon_1 + \alpha_2^2\epsilon_2 + \alpha_1\alpha_2\epsilon_6] - B_2\alpha_3^2\epsilon_3 - B_3\alpha_3^2(\epsilon_1 + \epsilon_2) + B_4(\alpha_2\alpha_3\epsilon_4 + \alpha_1\alpha_3\epsilon_5). \quad (2)$$

In the above equations, c_{ij}, ϵ_{i}, and α_{i} are the elastic constants, the strain components in the Voigt notation, and the direction cosines of the magnetization ($\vec{M}$), respectively. The axes 1, 2,

[a]Electronic mail: koch@pdi-berlin.de
[b]Permanent address: Malda College, Malda-732101, West Bengal, India.
[c]Permanent address: NTT Basic Research Laboratories, 3-1 Morinosato Wakamiya, Atsugi-shi, Kanagawa 243-0198, Japan.
[d]Present address: Specs GmbH, Voltastraße 5, 13355 Berlin, Germany.
[e]Present address: Solid State and Photonics Laboratory, Stanford University, Stanford, California 94305.

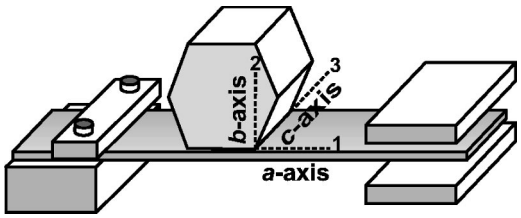

FIG. 1. Schematic illustration of our cantilever beam magnetometer using a lock-in assisted capacitance technique (right) to detect the substrate deflection; epitaxial configuration and orthogonal crystal axes of the hexagonal MnAs film deposited onto the GaAs(001) cantilever beam substrate are indicated.

and 3 correspond to the *a*, *b*, and *c* axes of the hexagonal crystal lattice, respectively, as illustrated in Fig. 1. Note that Eq. (2) differs from the ME energy density of Co derived by Bruno[18] due to the different demagnetized state, because the easy axis of magnetization of MnAs is along the *a* axis and not the *c* axis as for Co. The signs $(+/-)$ of all the terms in F_{mel} are consistent with Co yielding the same relation between the ME coupling constants (B_1, B_2, B_3, B_4) and the magnetostrictive constants (λ_A, λ_B, λ_C, λ_D). It is also noteworthy that the term $B_1\alpha_1\alpha_2\epsilon_6$ in Eq. (2) differs by a factor of 2 from the respective term of Co,[9,10] which seems to be due to an error upon interconverting tensor and Voigt notations.[10,18]

In the CBM experiments presented here the ME stress is measured for different states of magnetization (i.e., for different α_i). Stress σ_i is the partial derivative of the free energy with respect to the strain ϵ_i. The stress component σ_1 along the *a* axis of MnAs, which is parallel to the length of the cantilever beam and therefore measured in our CBM experiments, is given by

$$\sigma_1 = c_{11}\epsilon_1 + c_{12}\epsilon_2 + c_{13}\epsilon_3 + B_1(\alpha_1^2 - 1) - B_3\alpha_3^2. \tag{3}$$

Note that the in-plane strains (ϵ_1 and ϵ_3) remain constant during a magnetostriction measurement, because strong bonds to the substrate fix the lateral position of the film atoms. Only the strain perpendicular to the film plane ϵ_2 can change its value to minimize the free energy ($F=F_{\mathrm{el}}+F_{\mathrm{mel}}$). A magnetic field $\vec{H}$ that is high enough for saturation will align the magnetization $\vec{M}$ parallel to $\vec{H}$. For saturation magnetization along the three axes *a*, *b*, and *c*, σ_1 is calculated by

$$\vec{H} \| a\text{: } \alpha_1 = 1, \alpha_2 = \alpha_3 = 0$$

$$\sigma_1^a = c_{11}\epsilon_1 + c_{12}\epsilon_2 + c_{13}\epsilon_3, \tag{4}$$

$$\vec{H} \| b\text{: } \alpha_2 = 1, \alpha_1 = \alpha_3 = 0$$

$$\sigma_1^b = c_{11}\epsilon_1 + c_{12}(\epsilon_2 + \Delta\epsilon_2') + c_{13}\epsilon_3 - B_1, \tag{5}$$

$$\vec{H} \| c\text{: } \alpha_3 = 1, \alpha_1 = \alpha_2 = 0$$

$$\sigma_1^c = c_{11}\epsilon_1 + c_{12}(\epsilon_2 + \Delta\epsilon_2'') + c_{13}\epsilon_3 - B_1 - B_3. \tag{6}$$

In Eq. (4) the ϵ_i are strains due to the growth process, thermal expansion or, in the case of MnAs/GaAs(001), due to the structural phase transition, having no magnetostrictive contributions. $\Delta\epsilon_2'$ in Eq. (5) and $\Delta\epsilon_2''$ in Eq. (6) are the magnetostrictive components along the *b* axis, which can be calculated by setting the stress perpendicular to the film plane $\sigma_2=0$. Using an experimental geometry with the *a* axis of MnAs being parallel to the cantilever beam axis, the ME coupling constants B_1 and B_3 can be obtained by the following relations:

$$\sigma_1^b - \sigma_1^a = -B_1(1 + c_{12}/c_{11}), \tag{7}$$

$$\sigma_1^c - \sigma_1^a = -B_1 - B_3(1 - c_{12}/c_{11}). \tag{8}$$

In the case of MnAs, $c_{11}=49$ GPa and $c_{12}=12$ GPa (from Ref. 19).

III. EXPERIMENT

A 60 nm MnAs film on GaAs(001) was prepared as described elsewhere.[20,21] It grows predominantly (~95%) in the *A* orientation, i.e., with the hexagonal plane of MnAs, i.e., MnAs(0001), perpendicular to the GaAs(001) substrate and one of its *a* axes (namely, MnAs$[11\bar{2}0]$) and the *c* axis (i.e., MnAs[0001]) parallel to GaAs$\langle 110\rangle$.[22] In addition, the film contains small amounts of MnAs in the *B* orientation[22] (azimuthally rotated by 90°) as well as a tiny fraction with an out-of-plane magnetization.[23,24] The easy axis of magnetization is the *a* axis in the film plane.[25–27] The anisotropy fields are large, namely, 2.1 T in-plane along the *c* axis and 1 T out of plane, i.e., along the *b* axis (MnAs$[\bar{1}100]$) in accordance with Refs. 24 and 26.

The measurements were performed with our sensitive CBM,[7] which we used in the past for the quantitative determination of stress,[28] magnetization,[23,27] and magnetoelastic coupling[8,29] of epitaxial films. The magnetic fields are provided by two external magnets, an electromagnet yielding up to ±1.9 T as well as Helmholtz coil oriented perpendicular to the electromagnet with a maximum field of ±20 mT. The CBM is mounted on a versatile UHV manipulator and can be rotated along and perpendicular to the cantilever beam axis. 25×5 mm^2 sized samples served as cantilever beam substrates with the films covering an area of 11×5 mm^2. The MnAs film was oriented with the *a* axis of MnAs parallel to the length and accordingly the *c* axis along the width. The deflection of the free end of the cantilever beam was determined by a highly sensitive capacitance technique combined with lock-in-assisted signal detection. For calibration of the CBM, the deflection of the substrate due to its weight was measured while rotating the sample holder by 180°. The presented experimental data have been acquired at 10 °C, where the MnAs film is in its ferromagnetic α phase.[27]

The stress σ was calculated from the deflection using the following relation:[7]

$$\sigma = -\frac{E_s t_s^2}{6(1-\nu_s^2)t_f}\left(\frac{1}{R_l} + \nu_s\frac{1}{R_w}\right), \tag{9}$$

where E_s, ν_s, and t_s are Young's modulus, Poisson's ratio, and thickness of the substrate, respectively, t_f denotes the film thickness, and R_l and R_w are the radii of curvature along the length and the width of the cantilever beam substrate in the film region, respectively. We remark that due to the high

length-to-width ratio of our cantilever beam (>4) with the film starting about 5 mm away from the clamping position, we can treat bending as that of a free plate.[30–32] Length and width are oriented along different GaAs⟨110⟩ directions, where $\nu_s \approx 0$. Therefore Eq. (9) simplifies to

$$\sigma = -\frac{E_s t_s^2}{3 t_f l_f^2}\Delta. \tag{10}$$

We used $1/R_l \approx 2\Delta/l_f^2$ with l_f being the film length. Note that l_f enters Eq. (10), because the lengths of film and substrate are different. Δ is the substrate deflection at the end of the film. For measurement of B_1 of MnAs, magnetic fields between ±1.9 T parallel to the *b* axis are applied [Eq. (7)]. $\sigma_1^b(H) - \sigma_1^a$ is calculated by Eq. (10) from the difference in deflection with and without a perpendicular magnetic field. Note that in zero field $\vec{M}$ is parallel to *a*, which is the easy magnetization direction with strong magnetocrystalline anisotropy along *b* and *c*. Similarly, B_3 is obtained by applying $\vec{H} \| c$ and using B_1 [cf. Eq. (8)].

IV. RESULTS AND DISCUSSIONS

A. Experimental results

Figures 2(a) and 2(b) show the evolution of stress in MnAs/GaAs(001) arising when magnetic fields up to ±1.9 T are applied parallel to the *b* and *c* axes, respectively. As discussed above, each of the experimental data points was determined from the change in deflection when turning the magnetic field along the *b* or *c* axis on and off corresponding to $\sigma_1^b(H) - \sigma_1^a$ [Fig. 2(a)] or $\sigma_1^c(H) - \sigma_1^a$ [Fig. 2(b)], respectively. The stress curve of Fig. 2(a) reveals a complex behavior passing a maximum before it approaches a constant value at fields above 1 T. The curve of Fig. 2(b), on the other hand, reflects typical ME behavior with the ME stress being almost zero at low fields and increasing at higher fields until the film is eventually magnetically saturated. We remark that our available fields (±1.9 T) are slightly smaller than the saturation field along the hard *c* axis of MnAs [2.1 T according to our SQUID (superconducting quantum interference device) measurements]. For comparison, we include analogous measurements of an epitaxial Fe(001) film [Fig. 2(c)], which exhibits easy magnetization directions along [100] and [010]. Since they are parallel to the length and width of MgO(001) substrate, the film magnetization, which initially lies along the length, switches parallel to the width once the small in-plane coercive field (≈1 mT) is overcome. Obviously, both experiments with in-plane fields show the expected simple field dependence of the ME stress contribution, in contrast to Fig. 2(a). The finding is—at first sight—the more surprising as the curve of Fig. 2(b) includes also the ME coupling constant B_1 measured in Fig.2(a). The results of Fig. 2 therefore suggest that other effects are involved in addition to the ME coupling, when the magnetic field is applied perpendicular to the film plane.

B. Torque effect

It is well known that magnetic dipoles and accordingly magnetic thin films experience a torque $\vec{T} = V_f \vec{M} \times \vec{B}$ in external magnetic fields $\vec{B} = \mu_0 \vec{H}$ with V_f being the film volume. Applying $\vec{H}$ perpendicular to the film plane (*b* axis) rotates $\vec{M}$ from its easy magnetization direction along the length of the cantilever beam (*a* axis) gradually to the *b* axis and gives rise to a bending moment T_b along the width of the cantilever beam (*c* axis). The corresponding beam deflection Δ is calculated by[7]

$$T_b = -\mu_0 V_f H M \sin\theta = \frac{E_s w_s t_s^3}{6 l_f^2}\Delta \tag{11}$$

with θ denoting the angle between $\vec{H}$ and $\vec{M}$, and $M \sin\theta$ is the component of magnetization along the cantilever beam axis. According to Eq. (11), Δ depends linearly on *B* for small fields, where $\vec{M}$ lies still along the easy axis in the film plane, i.e., $\theta \approx 90°$ and $\sin\theta \approx 1$. A linear decrease of Δ (in unit of stress) is indeed observed in the range from −300 to +80 mT with a change of sign when the direction of *B* is reversed. The magnetization calculated from the slope in Fig. 2(a) is 0.68±0.05 MA/m, which is in good agreement with the bulk value. At $B \sim 80$ mT there is a jump in the curve from negative to positive values, which on further increase of *B* gradually approaches the initial slope of the

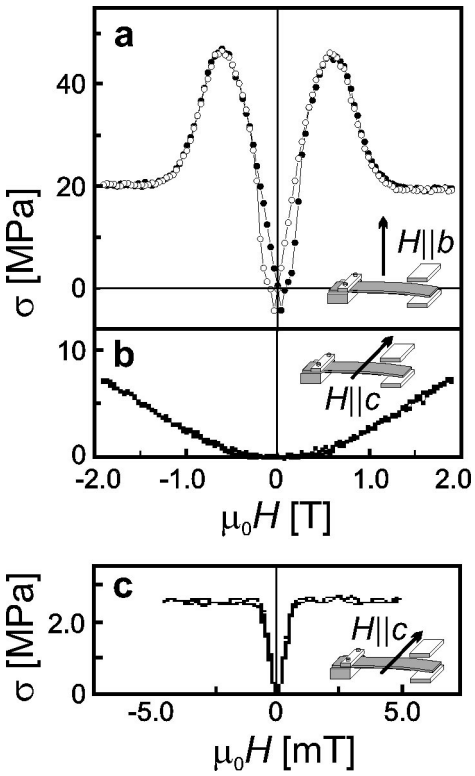

FIG. 2. Stress evolution (σ) upon applying perpendicular magnetic fields (H), measured by CBM: (a) 60 nm MnAs/GaAs(001), initial magnetization direction is easy *a* axis along the cantilever beam length, magnetizing field $\vec{H}$ is applied perpendicular to the film plane (*b* axis of MnAs); increasing (decreasing) $\vec{H}$ denoted by open (filled) dots. (b) 60 nm MnAs/GaAs(001), initial magnetization direction is easy *a* axis along the cantilever beam length, magnetizing field $\vec{H}$ is applied in the film plane along the cantilever beam width (*c* axis of MnAs). (c) 100 nm Fe/MgO(001) with easy axes parallel to length and width of the cantilever beam (see Ref. 33); initial magnetization direction is along the cantilever beam length, magnetizing field $\vec{H}$ is applied in the film plane along the cantilever beam width.

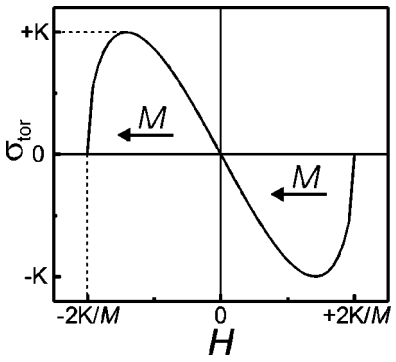

FIG. 3. Magnetic field dependence of the torque effect in cantilever beam experiments calculated by Eq. (14).

curve but with opposite sign. An analogous behavior is observed when sweeping the field back. As discussed in detail in Ref. 23 this unexpected slope reversal is due to a reversal of the in-plane magnetization. As confirmed by SQUID magnetometry[24] the MnAs film contains a small fraction with an out-of-plane magnetization that is magnetically coupled to the in-plane magnetization of α-MnAs film. Due to the magnetic coupling the in-plane magnetization can be switched not only by an in-plane field as usual but also by an out-of-plane field.

At higher magnetic fields (>300 mT) $\vec{M}$ is gradually rotated into the direction of $\vec{H}$. Since the component of $\vec{M}$ along the cantilever beam axis $M \sin\theta$ decreases, the bending moment due to the torque effect becomes smaller. In order to calculate the field dependence of the torque effect we assume the following expression for the free energy:

$$F(H) = -\mu_0 HM \cos\theta - K \sin^2\theta. \tag{12}$$

The constant K accounts for the contributions of both magnetocrystalline and shape anisotropy. We did not include ME effects into Eq. (12), because they can be separated from the torque effect by a proper design of the experiment (see Sec. IV C). Minimizing $F(H)$ with respect to θ and inserting into Eq. (11) yield

$$T_b = -\mu_0 V_f MH \sqrt{1 - \left(\frac{MH}{2K}\right)^2}. \tag{13}$$

With Eqs. (10) and (11) the field dependence of the stress due to the torque effect is obtained:

$$\sigma_{tor}(H) = \frac{2\mu_0 V_f}{w_s t_s t_f} MH \sqrt{1 - \left(\frac{MH}{2K}\right)^2}. \tag{14}$$

Note that M in Eqs. (13) and (14) can be positive or negative depending on the direction of $\vec{M}$. In Fig. 3, σ_{tor} is plotted as a function of the perpendicular field H with the film magnetization being negative (e.g., $-M$ pointing to the left). The progression of the curve exhibits two characteristic features.

(i) At small magnetic fields, when $(MH/2K)^2 \ll 1$, σ_{tor} depends linearly on H with the slope being proportional to M. The involved error in magnetization measurements is less than 1% as long as the probing field is below 10% of the saturation field. In previous experiments the probing field was typically less than 1%, thus confirming that CBM indeed is a precise magnetometer.

(ii) At higher fields the curve passes a maximum and then drops quickly to zero. The magnetic field at which the torque effect disappears ($H_0 = 2K/M$) as well as the magnetic field at the maximum of the curve ($H_{max} = \sqrt{2K/M}$) can be used to determine the respective anisotropy constant K. Therefore the two important magnetic parameters M and K are provided by the torque effect in hard axis CBM experiments.

For $\mu_0 H_{max} = 0.60$ T, taken from Fig. 2(a), a value of 0.29 MJ/m^3 is obtained for the anisotropy constant, which is in perfect agreement with the magnetostatic energy calculated for the MnAs film (0.29 MJ/m^3). The good agreement between anisotropy and magnetostatic energy implies that the magnetocrystalline energy within the hexagonal plane of MnAs is nearly isotropic, a result that is corroborated by a recent ferromagnetic resonance study.[34]

C. Separating torque effects from ME coupling

In the range of ±300 mT the magnetization of the MnAs film lies mainly along the easy axis, i.e., $\sin\theta \simeq 1$. At such small fields the ME coupling therefore is negligible. At higher fields, when $\vec{M}$ gradually is rotated into the direction of $\vec{H}$, the contribution of the ME coupling increases with increasing field, while the torque effect at the same time decreases. Ideally, the observed stress change at magnetic fields high enough to overcome the perpendicular anisotropy of the film (≈1 T for MnAs, Ref. 26) is solely magnetoelastic, since the torque effect is zero for $\vec{M} \| \vec{H}$.

In order to separate the ME coupling from torque effects in CBM experiments, we take advantage of the fact that the sign of the torque is determined by the sign of M, i.e., $\sigma_{tor}(+M) = -\sigma_{tor}(-M)$ [cf. Eq. (14)], whereas the ME coupling depends on M^2 (Ref. 17) with $\sigma_{mel}(+M) = \sigma_{mel}(-M)$. Therefore the total stress change $\sigma_{tot}(\vec{M}) = \sigma_{tor}(\vec{M}) + \sigma_{mel}(\vec{M})$ arising upon ramping the perpendicular magnetic field depends on the direction of $\vec{M}$ with respect to the cantilever beam. The experiment shown in Fig. 4 was designed to establish a well-defined orientation of $\vec{M}$. By tilting the perpendicular field slightly, by +4°, in direction of the cantilever beam axis, the in-plane component of $\vec{M}$ is kept positive by positive fields and negative by negative fields (see the inset of Fig. 4). According to Eq. (14), σ_T is positive in both cases (curve 1 in Fig. 4). The opposite is true for $\vec{H}$ tilted by −4°. Then the in-plane component of $\vec{M}$ is kept positive (negative) by negative (positive) fields corresponding to negative σ_T (curve 2 in Fig. 4). Adding curves 1 and 2 and dividing the result by 2 therefore eliminate the torque effect and yield $\sigma_{mel}(H)$ plotted as curve 3 in Fig. 4. On the other hand, by subtraction of curve 2 from curve 1 and division by 2 the pure torque effect is obtained.

We want to emphasize that the proposed method for separating torque and ME effects is applicable to any ferromagnetic material, as the selection of the magnetization direction of the film is achieved by the in-plane component of

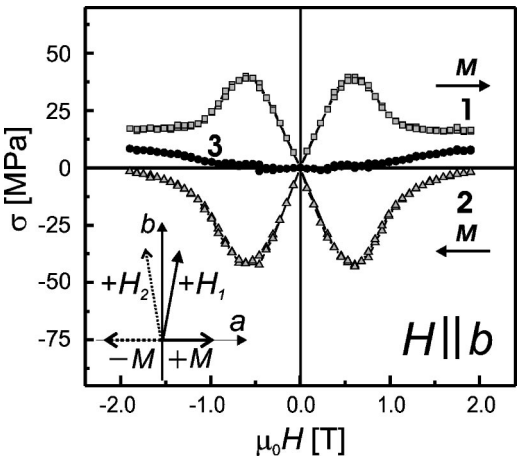

FIG. 4. Method of separating the magnetoelastic coupling from torque effects in cantilever beam experiments, where the film magnetization is rotated out of the film plane (see Sec. IV C for details): Curves 1 and 2 correspond to the involved stress change when the magnetizing field is tilted by +4° (H_1) and −4° (H_2) against the film normal, respectively. Adding curves 1 and 2 and dividing the results by 2 eliminate torque effects and yield the magnetoelastic stress as a function of H plotted as curve 3; note that curve 3 reveals the same field dependence of the stress as the curve in Fig. 2(b).

the tilted magnetic field. In the case of the MnAs film the switching thresholds between $-M$ and $+M$ are modified by the coupled out-of-plane magnetization component [not resolved in Fig. 4 due to the reduce data-point density compared with Fig. 2(a)], but the overall behavior at higher fields follows the general behavior. Furthermore, the proposed method works also when the easy axis of magnetization is perpendicular to the film plane and the magnetizing field lies in the film.

The ME coupling constant B_1 obtained from curve 3 of Fig. 4 at 1.9 T is −6.6 MPa(=MJ/m^3). Assuming saturation at 2.1 T for the hard-axis experiment of Fig. 2(b) as shown by SQUID, a value of 8.1 MPa is obtained for $\sigma_1^c - \sigma_1^a = -B_1 - B_3(1 - c_{12}/c_{11})$. Inserting B_1 yields $B_3 = -2.0$ MJ/m^3.

D. Other effects

It is worthy to discuss the torque effect of the MnAs film at high magnetic fields in more detail. In Sec. IV B it was shown that σ_{tor} is zero at fields above saturation. However, $\sigma_{\text{tor}} = \sigma - \sigma_{\text{mel}}$ of Fig. 4 assumes a finite value contrary to the model predictions. One possible explanation might be the pole effect, discussed in Ref. 12. When a ferromagnet is placed in a uniform magnetic field the magnetization tries to align parallel to the magnetic field by rotating the magnetization as described in Sec. IV B and/or by rotating the magnet itself (like a compass needle). In our experimental setup the ferromagnetic film is attached to the substrate. It is therefore not free to rotate, but it can bend. Assuming a pole effect, the magnetocrystalline anisotropy energy could be reduced by a bending of the beam, say by an angle θ', while keeping $\vec{M}$ still parallel to $\vec{H}$. By this means the magnetocrystalline anisotropy energy is reduced, but elastic energy has to be spent for bending. The equilibrium value of θ' is obtained by minimization of the total energy (elastic and anisotropy) of the sample. Since both the magnetic contribution to the elastic energy[12] and the anisotropy energy [Eq. (12)] vary with θ'^2, the total energy of the system will be minimum at $\theta' = 0$. Thus the pole effect cannot explain the additional deflection of the CBM.

The additional stress contribution observed in Fig. 4 is most likely due to a small fraction of material within the α-MnAs matrix that exhibits a tilted magnetization (see Ref. 24). Analogous to α-MnAs, the in-plane component of the tilted fraction gives rise to a torque in a perpendicular field (see Sec. IV B). In fact, the occurrence of a torque effect in perpendicular fields corroborates our previous presumption that its magnetization is tilted, thus exhibiting both an in-plane and an out-of-plane component. It therefore can be switched by an out-of-plane field and at the same time be magnetically coupled with the in-plane magnetization of α-MnAs. The magnetocrystalline anisotropy energy of this additional magnetic fraction is very high, since its magnetization is not aligned with the perpendicular magnetic field even at a field strength as high as ±1.9 T. In our recent study[24] we also found that its critical temperature, at which ferromagnetic order disappears, is much higher than that of α-MnAs. However, since the additional stress contribution is due to a torque effect, it is an odd function with respect to $\vec{M}$ and therefore can be separated from the ME coupling by the procedure described in Sec. IV C.

V. CONCLUSION

In order to quantitatively determine the ME coupling constant of thin films with a CBM we investigated the stress evolution upon applying magnetic fields perpendicular to the film plane. Contrary to the commonly used experimental geometries, where the magnetizing field lies in the film plane, a complex dependence of the stress on the magnetic field is observed, when the film magnetization is rotated out of the film plane. Our analysis reveals that the involved stress contains two contributions: (i) stress due to the ME coupling and (ii) stress due to torque which the film—as a magnetic dipole—experiences in perpendicular fields. Whereas ME stress is an even function with respect to $\vec{M}$, torque effects are odd functions. Taking advantage of the different symmetries we proposed a simple method to separate ME coupling and torque effects by using magnetic fields that are slightly tilted against the film normal. Depending on the sign of the tilt angle, the film magnetization is either kept positive or negative by the applied field and therefore cancels out when the signals of both experiments are added. The proposed method for separating torque and ME effects is applicable to any ferromagnetic material, as the selection of the magnetization direction of the film is achieved by the in-plane component of the tilted magnetic field. It works as well for thin film systems with out-of-plane easy axis. In that case the magnetizing field is applied in the film plane along the cantilever beam axis. Furthermore, we showed that from the torque effect appearing in hard axis CBM experiments both the film magnetization and the respective anisotropy constant K can be quantitatively determined. All in all, cantilever

beam magnetometry is a powerful technique for studying the magnetic properties of thin films, particularly when considering also the high sensitivity of the method.

ACKNOWLEDGMENTS

We thank L. Däweritz for providing the MnAs/GaAs(001) sample and carefully reading the manuscript. The work was supported by the Deutsche Forschungsgemeinschaft (Grant No. Sfb 290) and the NEDO International Joint Research Program "Nanoelasticity."

[1]R. Becker and W. Döring, *Ferromagnetismus* (Springer, Berlin, 1939).
[2]Charles Kittel, Rev. Mod. Phys. **21**, 541 (1949).
[3]E. du Trémolet de Lacheisserie, *Magnetostriction: Theory and Applications of Magnetoelectricity* (CRC, Boca Raton, FL, 1993).
[4]S. W. Sun and R. C. OHandley, Phys. Rev. Lett. **66**, 2798 (1991).
[5]E. Klokholm, IEEE Trans. Magn. **12**, 819 (1976).
[6]A. C. Tam and H. Schroeder, J. Appl. Phys. **88**, 5422 (1988).
[7]M. Weber, R. Koch, and K. H. Rieder, Phys. Rev. Lett. **73**, 1166 (1994).
[8]G. Wedler, J. Walz, A. Greuer, and R. Koch, Phys. Rev. B **60**, R11313 (1999).
[9]D. Sander, Rep. Prog. Phys. **62**, 809 (1999).
[10]Th. Gutjahr-Löser, D. Sander, and J. Kirschner, J. Magn. Magn. Mater. **220**, L1 (2000).
[11]E. van de Riet, J. Appl. Phys. **76**, 584 (1994).
[12]E. du Trémolet de Lacheisserie and J. C. Peuzin, J. Magn. Magn. Mater. **136**, 189 (1994).
[13]E. Klokholm and C. V. Jahnes, J. Magn. Magn. Mater. **152**, 226 (1996).
[14]E. du Trémolet de Lacheisserie and J. C. Peuzin, J. Magn. Magn. Mater. **152**, 231 (1996).
[15]P. M. Marcus, Phys. Rev. B **53**, 2481 (1996); Phys. Rev. B **54**, 3662 (1996).
[16]P. M. Marcus, J. Magn. Magn. Mater. **168**, 18 (1997).
[17]W. P. Mason, Phys. Rev. **96**, 302 (1954).
[18]Patrick Bruno, J. Phys. F: Met. Phys. **18**, 1291 (1988).
[19]M. Dörfler and K. Bärner, Phys. Status Solidi A **17**, 141 (1973).
[20]M. Kästner, C. Herrmann, L. Däweritz, and K. H. Ploog, J. Appl. Phys. **92**, 5711 (2002).
[21]F. Schippan, A. Trampert, L. Däweritz, and K. H. Ploog, J. Vac. Sci. Technol. B **17**, 1716 (1999).
[22]L. Däweritz, M. Ramsteiner, A. Trampert, M. Kästner, F. Schippan, H.-P. Schönherr, B. Jenichen, and K. H. Ploog, Phase Transitions **76**, 445 (2003).
[23]C. Pampuch, A. K. Das, A. Ney, L. Däweritz, R. Koch, and K. H. Ploog, Phys. Rev. Lett. **91**, 147203 (2003).
[24]A. Ney, T. Hesjedal, C. Pampuch, J. Mohanty, A. K. Das, L. Däweritz, R. Koch, and K. H. Ploog, Appl. Phys. Lett. **83**, 2850 (2003).
[25]M. Tanaka, J. P. Harbison, M. C. Park, Y. S. Park, T. Shin, and G. M. Rothberg, J. Appl. Phys. **76**, 6278 (1994).
[26]F. Schippan, L. Däweritz, G. Behme, K. H. Ploog, B. Dennis, K.-U. Neumann, and K. R. A. Ziebeck, J. Appl. Phys. **88**, 2766 (2000).
[27]A. K. Das, C. Pampuch, A. Ney, T. Hesjedal, L. Däweritz, R. Koch, and K. H. Ploog, Phys. Rev. Lett. **91**, 087203 (2003).
[28]R. Koch, in *The Chemical Physics of Solid Surfaces*, Growth and Properties of Ultrathin Epitaxial Layers, Vol. 8, edited by D. A. King and D. P. Woodruff (Elsevier Science, Amsterdam, 1997), pp. 448–489.
[29]R. Koch, M. Weber, K. Thürmer, and K. H. Rieder, J. Magn. Magn. Mater. **159**, L11 (1996).
[30]D. Krus, Jr., G. Mearini, K. Chaffee, and R. W. Hoffman, J. Vac. Sci. Technol. A **9**, 2488 (1991).
[31]K. Dahmen, S. Lehwald, and H. Ibach, Surf. Sci. **446**, 161 (2000).
[32]K. Dahmen, H. Ibach, and D. Sander, J. Magn. Magn. Mater. **231**, 74 (2001).
[33]G. Wedler and R. Koch (unpublished).
[34]J. Lindner, T. Tolinski, K. Lenz, E. Kosubek, K. Baberschke, A. Ney, T. Hesjedal, C. Pampuch, R. Koch, L. Däweritz, and K. H. Ploog, J. Magn. Magn. Mater. **277/1–2**, 159–164 (2004).